

# AN INVESTIGATION OF SIDE IMPACT TEST METHODOLOGIES FOR CHILD RESTRAINT SYSTEMS USING FINITE ELEMENT SIMULATIONS

**Jesus Monclus-Gonzalez**

Royal Automobile Club of Spain

Spain

**Dhafer Marzougui**

**George Bahouth**

**Azim Eskandarian**

FHWA/NHTSA National Crash Analysis Center

United States

Paper Number 121

## ABSTRACT

A Finite Element (FE) model of a convertible forward-facing Child Restraint System (CRS), presented in a 2001 ESV paper has been combined with a Hybrid III 3-year-old dummy model and an ECE44R test bench model. The combination will replicate the last ISO proposal for side impact tests of CRS in order to analyze the influence of the longitudinal acceleration pulse seen during FMVSS 214 tests. This influence is shown to be limited, as long as the dummy is confined within the CRS shell. In agreement with previous crash investigations, the simulated intruding door in the ISO proposal is responsible for a large share of the loads acting on the child dummy. The validation of the virtual model and limitations of the child dummy FE model are discussed. Simulation results are compared with an actual frontal test using the same CRS model.

## INTRODUCTION

Laboratory testing has been the traditional approach when it comes to automobile safety research. However, one of its disadvantages is that laboratory dynamic testing focuses on a single crash type and crash severity, while real-life crashes tend to be a complex phenomenon with pre and post crash relevant events. Furthermore, data measured on dummies allow only limited conclusions about real world crash behavior and potential injuries of children. Finally, laboratory conditions are limited and therefore coping with the widespread CRS misuse seen in the real world is difficult [1].

Simulation represents a useful complementary tool to traditional testing both in industry and research environments. In industry, the main purpose of simulation is to test designs at an early stage in the pre-prototype development process and before they are actually crash tested. Simulation can reduce the number of tests required to evaluate the performance

of a system. As for the research community, simulation can be invaluable when analysing an existing or hypothetical scenario or design. In connection with a recognized present and future problem, simulation can improve the former and solve the latter. More complex scenarios can be approached in the computer without having to develop and validate expensive laboratory devices.

A limited number of computer simulations using rigid body based MADYMO software [2] has been reported in related literature [3, 4, 5]. Rigid body simulations are not computationally expensive. They present themselves as a valuable tool in gaining insight into the relationship of the various parameters. The Finite Element technique could be situated halfway between real testing and rigid body simulations. In fact, the alliance between high performance-low cost computers and the last versions of finite element method codes have recently dawned many un-explored areas of research. Highly detailed finite element models can be used to develop simpler and faster rigid body representations of complex engineering problems [6].

In the vehicle safety field, lateral impacts continue to be a dominant risk for child passengers. About one third of the restrained children with AIS3+ injuries included in a European study were involved in side collisions [7]. A Swedish study has shown that approximately 50% of the fatally injured children, up to 3 years of age, occurred in side impacts [8]. Other studies concur with the significance of side impacts casualties as being on the same relevance as those occurring during frontal impacts [9, 10, 11, 12]. In the USA, Agran et al examined injury patterns in children aged 4 to 9 years who were restrained in motor vehicle crashes. Through a hospital-based monitoring system, it was found that MAIS2+ are more frequent in near-side impacts (41%) than in frontal (15%) and rear-end crashes (3%) [13]. This is not a child specific situation as a higher fatality rate

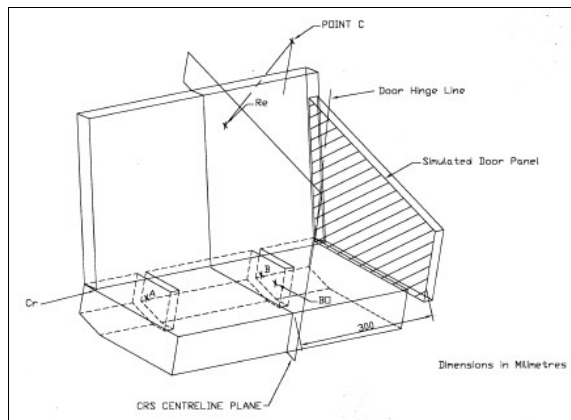
for adult occupants has also been recently presented [14]. Within the ISO/TC22/SC12/WG1 “Child Restraint Systems” an ad-hoc group was founded in 1993 to develop a test standard for side impact protection for restrained children [15].

One of the CRS Finite Element models presented in a previous ESV paper [16] has been combined with an existing Hybrid III 3-year-old child dummy FE model and an in-house developed ECE Regulation 44 [17] test bench model. It was exercised in various frontal (for validation purposes) and side impact scenarios. Throughout the research, special attention has been paid to the influence of the FMVSS 214 [18] struck vehicle longitudinal pulse when applied to the ISO proposal for CRS side impact testing.

### ISO PROPOSAL & FMVSS 214 CRASH PULSE

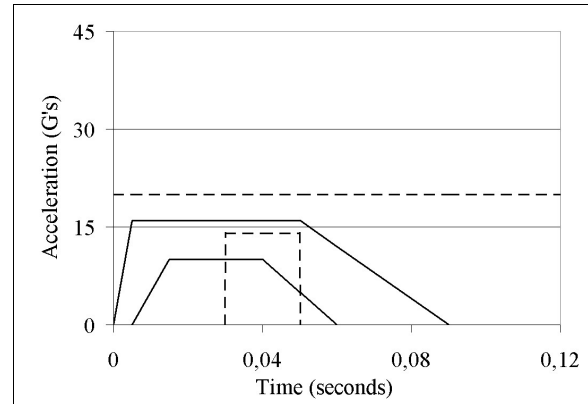
#### ISO CRS Side Impact Test Proposal

Thus far, regulation ECE R44 does not include any side impact tests. In fact, side impact sled tests are only described in Australian/New Zealand regulation AS-3629. Here, the CRS is mounted on a sled which is subjected to a 32 km/h change in velocity and where a fixed door simulates the vehicle’s structure [19]. In the above mentioned ISO proposal for side impact testing, the CRS is attached to a bench mounted on a sled. It is decelerated, thus reproducing the kinematics of the struck vehicle’s chassis. An intruding door is represented by a pivoted door structure. It is rotated, in relation to the test seat, at a relative angular velocity obtained from velocities measured in full-scale tests. This movement represents a v-shaped intrusion of the door’s inner panel. A perspective of the test bench and the hinged door is shown in Figure 1.



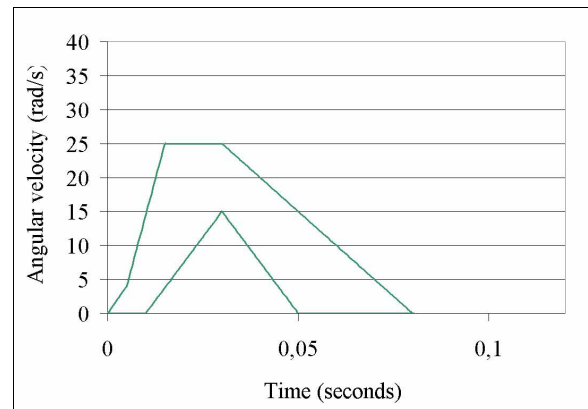
**Figure 1. Seat bench and hinged door proposal.**

Figure 2 shows the corridor for the sled deceleration. The side deceleration defined in the Australian regulation has been included in the graph to facilitate comparison between them. The sled’s velocity change in the ISO proposal reaches 25 km/h. This represents an impact of two vehicles of equal mass where the striking vehicle travels at 50 km/h.



**Figure 2. ISO (solid) - AS (dotted) sled corridors.**

The hinged door angular velocity profile should lie in the corridor represented in Figure 3. The velocity should not be affected by contact with the CRS. The maximum door angle for the rear facing CRS is 25°. For the forward facing seats, this maximum angle must still be specified by the ISO.



**Figure 3. ISO door angular velocity corridor.**

#### US Side NCAP longitudinal pulse

The ISO/TC22/SC12/WG1 N 504 CRS side impact test proposal does not include any sled longitudinal acceleration component. But, analysis of NASS data 1988-1997 shows that 10 and 2 o’clock are the most common injurious impact directions in vehicle to vehicle crashes. This could be indicative of a high longitudinal velocity change [20]. Also, in a paper by Langwieder et al, forward movement is deemed to be

present in 35% of all studied MAIS2+ CRS crashes [21]. This movement could be caused by pre-impact braking, by non-perpendicular collision angle or simply by the longitudinal  $\Delta v$  of the struck vehicle during impact. In Langwieder's paper, it is stated that "the influence of forward movement has to be analysed in further crash tests". In the case of child passengers, such a longitudinal component may cause the child dummy's head to move forward relative to the CRS and therefore be more exposed to impact with the intruding door, and consequently increase the risk of head injury.

An available source for determining realistic vehicle kinematics in different crash scenarios is full-scale crash tests. With respect to side crashes, the two major standards are US FMVSS 214 and European Directive 96/27/EC. The test procedures of both regulations are similar in that a stationary test vehicle is struck with a moving deformable barrier (MDB). However, they use different test procedures, barriers, dummies and injury criteria. Figure 4 shows the FMVSS 214 crash test configuration.

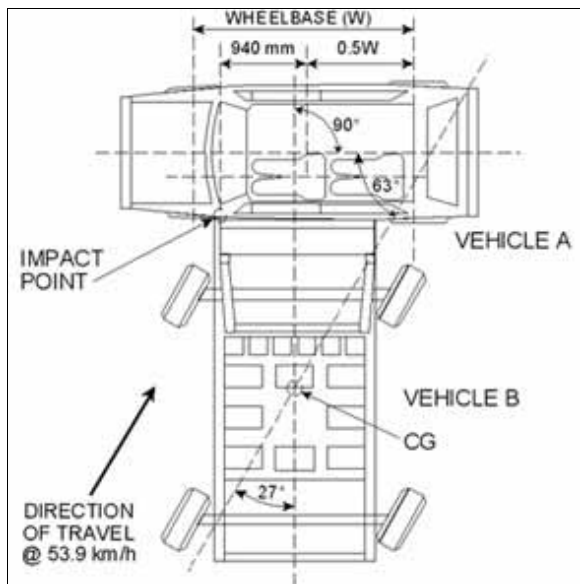


**Figure 4. FMVSS 214 crash configuration.**

As opposed to the European Directive which represents a 90° impact against a static vehicle, the FMVSS 214 dynamic test simulates the 90-degree impact of a striking vehicle travelling 48.3 km/h (30 miles per hour) into a target vehicle travelling perpendicularly at 24.2 km/h (15 mph). This is achieved in the American regulation by means of a moving deformable barrier with all wheels rotated 27 degrees (crab angle) from the longitudinal axis. The deformable barrier impacts a stationary test vehicle with a 54 km/h closing speed. On the contrary, and

because it is a purely perpendicular crash, European regulation 96/27/EC does not confer the struck vehicle any substantial longitudinal component, while FMVSS 214 does. As a conclusion, and at least with regard to this circumstance, the American regulation can be deemed as more realistic.

A variation of FMVSS 214 is represented by the US Side New Car Assessment Program (SNCAP). The only difference between these two crash test configurations is the impact velocity, which is raised to 62 km/h for SNCAP. The increase in impact velocity translates into a more demanding test and therefore highlights differences between vehicles and provides consumers with more useful information.

In order to investigate the influence of the longitudinal component of vehicles' deceleration during side impacts, a generic longitudinal crash pulse has been defined based on the analysis of a total of 11 SNCAP tests [22]. All of these crash tests correspond to compact car models, midsize passenger cars and minivans and have been selected bearing the following criteria: availability of good quality CG crash pulses; latest model years; and condition of worldwide vehicles (present in both US and European markets). Average crash test pulses have been calculated for each of the three vehicle classes and, as the last step, the components of the three vehicle categories have been averaged to obtain a generic crash pulse during Side NCAP tests. Figure 5 shows the generic pulse and compares it to the ISO proposed sled deceleration corridor.

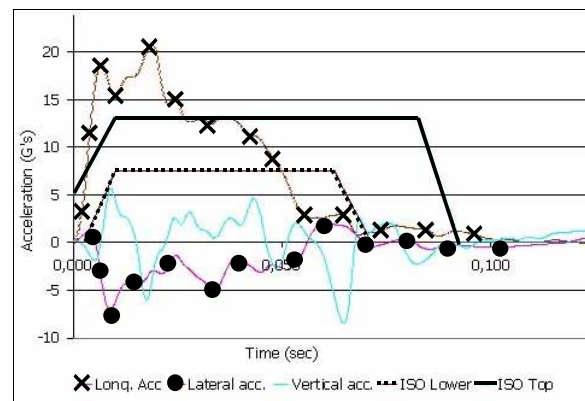


**Figure 5. Generic pulses in US SNCAP tests.**

The longitudinal component is shown isolated in Figure 6.

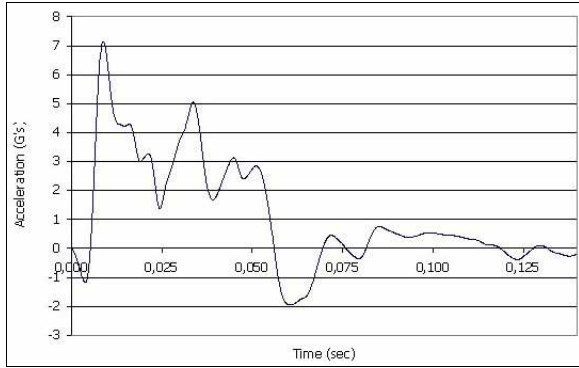


**Figure 6. Generic longitudinal pulse in SNCAP.**

## FINITE ELEMENT MODEL DESCRIPTION

### CRS FE model selection

Booster seats normally offer a much smaller protection during side impacts than other types of CRS unless they have high-backs with large side wings. High-backs and large side wings protect the head and thorax from direct impact with the vehicle's structures. On the opposite end of the spectrum, infant seats normally achieve a much better level of protection during side impacts. This is true if they have an adequately reinforced, large shell and proper padding. Between these two types of CRS, forward facing child restraint systems should be able to sufficiently protect their occupants during side crashes. However, the interaction between the child and the harness or other restraining method (frontal tray or shield, for instance) is complex enough to pose doubts on the level of exposure to impacts with the vehicle's (intruding in many cases) interior. In addition to this, the latest data from the Children's Hospital in the USA also point out that in side impacts where the child passenger suffered serious injuries, forward facing CRS are the most frequent CRS configuration, as shown in next Figure 7 [23].

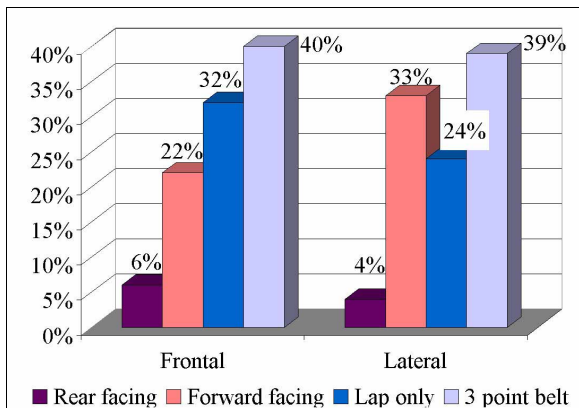


**Figure 7. Distribution of CRS types in Children's Hospital database.**

Table 1 shows the age distribution of fatalities in the USA, disaggregated by restraint use and covering a period of three years [24]. The predominance of the 1-4-year-old group is clear in that the forward facing CRS is the most adequate CRS for this age group.

**Table 1. Distribution of child fatalities by CRS type**

CRS Type	Age < 1	Age 1-4	Age 5-6	Total
None	222	756	353	1,331
L/S Belt	2	117	84	203
Lap Belt	13	159	138	301
Child Seat	255	428	12	695
Total	492	1,460	587	2,539

Langwieder et al also analyzed the age of the subjects in side impact crashes. Ejections, non-use of of CRS and massive intrusion was eliminated from the database [21].

**Table 2. Age distribution in side impacts in Europe**

Age	Total n	Total %	Subset n	Subset %
0-1	42	31%	14	21%
2-3	33	24%	14	21%
4-5	16	12%	11	16%
6-7	16	12%	9	13%
8-9	14	10%	9	13%
10-11	16	12%	11	16%

When studying side impacts in the UK, Thomas and Frampton came to the conclusion that children 0-3 years showed a relatively higher injury risk [14]. In his study, Langwieder et al also found that children under 4 years had an increased injury risk.

It can therefore be concluded that in diverse geographical areas, forward facing convertible seats are called to play a remarkably important role in the protection of children in side and frontal crashes.

For all these reasons, one convertible CRS FE model (previously developed by the authors in LS-DYNA [16]) was selected for further investigation of side impacts. Using FE simulations, the objective was to gain insight into the influence of the side impact longitudinal pulse. Figure 8 and 9 show the actual seat before disassembling it for analysis purposes and an exploded view of its FE model (basic statistics of this model are included in Appendix 1).



**Figure 8. Photograph of the selected CRS.**

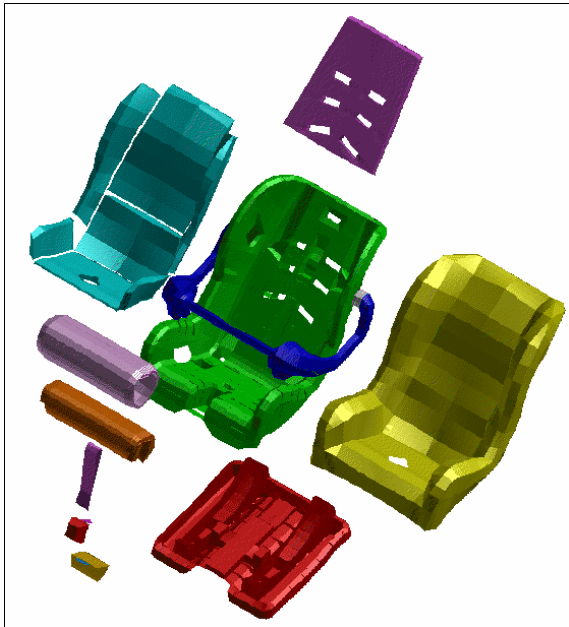


**Figure 9. Components of the CRS FE model.**

### **FE Dummy Model Description**

First Technology Safety Systems (FTSS) is a dummy manufacturer located in the Detroit area (Michigan, USA) which also generates FEM models of its products [25]. One of these available dummy models has been chosen for this research: the H3-03 Version 2.3beta2 [26]. This model of the Hybrid III 3-year-

old dummy was developed in cooperation with Ove Arup & Partners Detroit Limited [27].

Geometry for this model was taken from the engineering drawings for the machined parts. Three-dimensional scans were made of the aluminium and brass castings, such as the skull, pelvis bone and femur hip joints. The vinyl and foam parts were scanned from the production molds or master patterns. Model masses and inertias were checked against the production parts. Wherever practical, material properties were derived from material tests of samples made in special molds or sectioned from production parts. Non-deformable components, typically the skeleton, are modelled as rigid bodies but are accurate representations of the actual parts.

The articulation of the dummy components is allowed by LS-DYNA joints. A spherical joint is used when the physical joint is a ball-in-socket joint. A revolute joint is used when the physical joint acts as a hinge. The joints in this dummy are located in shoulders, elbows, knees, ankles, yokes and hips. A joint is also used at the neck load cell beams. Joints are also used for the chest deflection transducer: two revolute joints are used at the lower (spine box) end of the transducer arm and a cylindrical and a spherical joint are used at the upper (sternum) end.

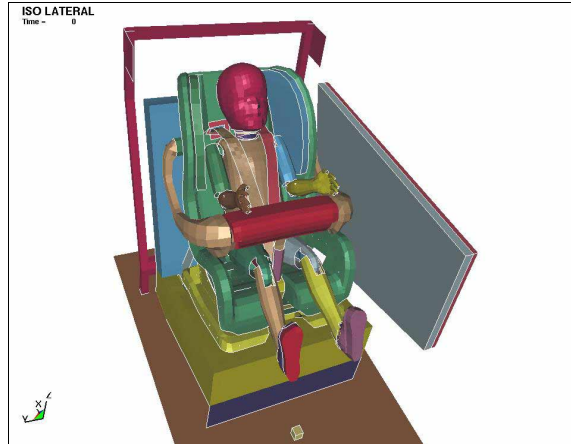
To collect the same data that can be obtained from the actual Hybrid III 3-year-old dummy, tri-axial accelerometers are mounted at three different locations in the FE model: head, chest and pelvis. Load cells are defined as zero length beams using LS-DYNA material type 66 elements in the following locations: upper neck, lower neck, pelvis and acetabulii (left and right). These act as stiff translational and rotational springs, as it actually happens in the actual dummy. Each load cell beam has a unique part, material and section ID and is located at the intersection of the load cell's neutral axes. The instrumentation is completed, as previously mentioned, with a chest deflection transducer. When the chest is compressed, the upper end of a rod pinned to an adapter at the base of the spine box slides up the sternum and a rotary potentiometer (modelled with a near-zero-stiffness rotational spring in LS-DYNA) measures the rotation of this rod.

### **Complete FE Model**

An LS-DYNA version of an ECE44R, which was developed by the authors, was finally combined with the convertible CRS FEM model and the Hybrid III 3-year-old model presented above. For the side impact simulations a hinged door has also been

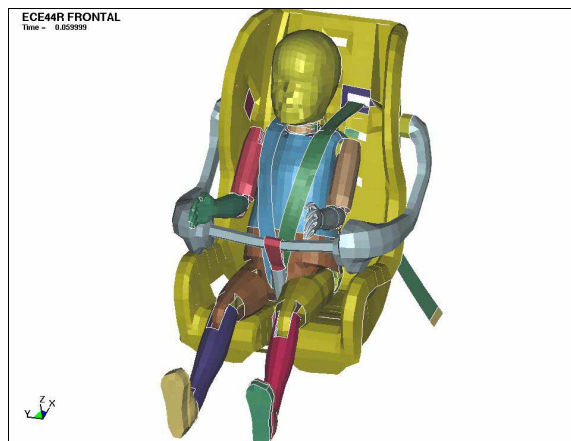
modelled following specifications included in the ISO/TC22/SC12/WG1 sled test proposal. The complexity of the complete frontal and lateral ECE44R bench, CRS and dummy FEM models are shown in Table A1 in Appendix 1.

Figure 10 shows the final configuration of the complete Finite Element model, in its side-impact version, with a simulated intruding door conforming to the ISO proposal.



**Figure 10. Test bench + CRS + dummy model.**

Two versions of the CRS harness were created. The first is a reduced version with the shoulder straps connected via a nodal rigid body constraint to the back of the CRS shell. The second includes all straps in the back of the CRS that were connected to the harness retractor. This connection is made by means of a discrete beam that allows force measurement in the harness. Also, this beam permits the definition of different slack conditions. The detailed version of the harness is shown in Figures 11 and 12.



**Figure 11. CRS-dummy model (frontal view).**



**Figure 12. CRS-dummy model (rear view).**

During the initial simulations, the following changes were progressively introduced in order to avoid computational problems such as negative volumes, hourglassing and shooting nodes in the FTSS Hybrid III 3-year-old FE dummy model:

- The part named “Thorax – Null Shells of Abdomen Foam Interior” was connected to the part “Thorax – Spine Box Rigid” with one extra node set to rigid body.
- Several nodes in the chest were moved forward 1.5 mm to avoid initial near-penetrations between parts “Thorax – Foam on Jacket Front” and “Thorax – Jacket Front Top” and “Thorax – BIB Contact Null”. The near-penetrations were considered to be contributing to the generation of negative volumes.
- A contact was added between nodes of “Thorax – Shoulder Ensolite Pad” and part “Thorax – Jacket Contact Null Inner”.
- A new contact definition was defined between parts “Thorax – Left Shoulder Bracket”, “Thorax – Right Shoulder Bracket”, “Thorax – Lower Neck Load cell Lower Rigid”, “Thorax – Lower Neck Load cell Upper Rigid” and “Thorax – BIB Contact Null” to better distribute contact forces in the shoulder/neck region. This area bears significant loads generated in the interaction with the harness straps and more attention may be necessary in future research.

## FE MODEL VALIDATION

Validation is somehow still a vague concept since it depends of the final purpose of the model. Once the purpose of the FEM model is defined, the validation goals can be stated and the model results can then be assessed by comparison with those targets. In many cases, simulation tends to focus less on the

performance of an individual vehicle or safety system and more on the characteristics of a vehicle class or type of restraint. On the other hand, a ten percent variability in real-life tests is also common and consequently admitted when comparing test and simulation results. For the purposes of this research, validation status will be defined as “the ability to replicate the general behavior of a child safety seat”. In this research, validation of the complete CRS+bench+dummy FE model was conducted by assessing both the realistic behavior of components during the simulation (CRS shell, CRS front shield, CRS harness, bench cushions, bench seatbelt, dummy...) and the relevant injury criteria measurements during a frontal simulation.

Figure A1 in Appendix 2 shows a sequence of pictures corresponding to a frontal simulation at 20 ms intervals. Two sets of injury criteria were used to validate the FE model. The first one is obtained from an actual sled test of the same CRS model under identical crash conditions using a Q3 dummy. The second is derived from a batch of frontal tests performed by the consortium EuroTest [28].

In general, the simulation shows a realistic overall kinematical behavior; however, head and knee excursion in the actual test are larger than those obtained in the simulation. Some reasons for this could be the following: influence of the bench seatbelt retractor; difference in dummy interaction with the CRS harness; and inaccuracy of material properties used in the CRS FEM model. During the real test, the Q3 dummy slouches more than the Hybrid III does during the simulation. In fact, in the actual test, the dummy’s head flexes forward and impacts the CRS front shield. This is not reproduced during the simulation even when the general neck/head trajectory is in agreement with that of the test prior to the contact. In order to further investigate these discrepancies, more details about the installation of the Q3 dummy in the test rig would be necessary.

As far as the numerical comparison, the main differences appear in the dummy’s head acceleration as previously explained. The contact between the head and the CRS front shield that happens during the actual test is not replicated in the simulation. There is good agreement in the chest accelerations between real and virtual tests. Pelvic data are less comparable and they should be carefully approached since these curves are more erratic both in test and simulation.

Table 3 summarizes the relevant biomechanical criteria for this simulation.

**Table 3.**  
**Injury values used for validation purposes**

Criteria	FE model	Test (same CRS)	EuroTest series
HIC36	661	842	283/997
Head max. res. Acc. (G, 3ms)	59	69	47/76
Head excursion (mm)	510	550	500/670
Neck max axial force (N, 3ms)	1846	2300	1472/2709
Chest max res. acc. (G, 3ms)	56	53	36/64
Chest max vert. acc. (G,3ms)	18	17	15/31

It should be pointed out that the actual test of this CRS was performed with a Q3 dummy. The differences between this dummy and the Hybrid III 3-year-old, whose FEM model has been used in the simulations, have been pointed by Berliner et al [29].

From Table 3, it is concluded that all relevant biomechanical measurements are comparable with the range of values in actual similar tests. For this reason, the ECE44R bench with convertible child safety seat and FTSS Hybrid III 3-year-old model is considered validated for the purposes of this research.

The frontal models were run on an SGI Origin 3800 supercomputer at the FHWA/NHTSA National Crash Analysis Center - NCAC. The 3800 computer series allows scaling up to 512 CPUs, using a system bandwidth of up to 716 GB/s and a maximum memory of 1 TB. The computer frame at the NCAC has 32 processors, an internal bus speed of 600 MHz, 8 MB cache, 8GB 2-way interleaved memory and an 800 GB fiber channel disk. The maximum performance of this hardware is 33.3 Gflops.

Computation time of a complete ECE44R bench with CRS and dummy FEM simulation run with a duration of 150 ms is shown in Table 4 and compared with two other machines: a PC with a Intel Pentium 4 processor at 1.50 GHz (with a cache of 256 KB, 256 MB of RDRAM and a bus speed of 100 MHz) and an SGI Origin 2000. The model used for CPU time benchmarking has the following summarized statistics: 129 connections, 34 contact definitions, 22254 shell elements, 9579 solid elements, 153 beams, 60 thick shell elements, 36 elements of other types, and 29114 nodes.

**Table 4.**  
**Computation time for a 150 ms frontal simulation**

Machine	Number of CPUs	Time (hh:mm:ss)
PC P-4	1	9:37:26
SGI 2000	4	7:41:39
SGI 3800	1	6:57:18
SGI 3800	2	4:38:48
SGI 3800	4	3:17:37
SGI 3800	6	2:45:05
SGI 3800	8	3:02:33
SGI 3800	16	3:10:02

### SIDE IMPACT SIMULATIONS

Once the model was deemed validated, and experience with the different features and limitations of the model and dummy injury criteria was accrued and the influence of the longitudinal deceleration, typically seen on FMVSS 214 lateral crash tests, was investigated. The longitudinal pulse defined above was added to the proposed ISO/TC22/SC12/WG1 sled side impact configuration. In addition to this longitudinal pulse, the crabbed sled test configuration, used in the 2002 edition of the EuroTest consumer information program, was reproduced both with and without an intruding door [30].

In the EuroTest consortium, the CRS is mounted on the rear seat bench of a VW Golf model year 2001 body in white which is installed on the sled. A simulated fixed door, similar to that of the ISO proposal, is added to the body in white. Figure 13 shows this lateral impact configuration.



**Figure 13. EuroTest lateral sled test.**

Table 5 shows the complete battery of investigated lateral simulations.

**Table 5.**  
**Battery of lateral simulations**

Simulation title	Description
ISO	Simulation according to ISO/TC22/SC12/WG1 N573. Reduced harness FEM model. “Baseline” simulation run.
ISO no door	Baseline simulation without hinged door. Similar to far side (non-struck side) conditions.
ISO only door	Baseline simulation without lateral pulse but with intruding door.
ISO no padding	Baseline simulation without lateral head padding in the CRS.
ISO 214	ISO proposal with average FMVSS 214 longitudinal pulse as previously described.
ISO 214x2	ISO proposal with average FMVSS 214 longitudinal pulse scaled by a factor of 2, run on a single processor.
ISO 214x2b	Same as before with different number of processors (four) to check for consistency of result.
ISO 214x2 10019	ISO proposal with average FMVSS 214 longitudinal pulse scaled by a factor of 2. Fabric material used for the seatbelt.
ISO 214x2 new harness	ISO proposal with average FMVSS 214 longitudinal pulse scaled by a factor of 2. Detailed harness model.
ISO 214x2 no harness	ISO proposal with average FMVSS 214 longitudinal pulse scaled by a factor of 2. Gross misuse simulation: dummy not strapped in the CRS).
ISO 214x3	ISO proposal with average FMVSS 214 longitudinal pulse scaled by a factor of 3.
ISO 214x4	ISO proposal with average FMVSS 214 longitudinal pulse scaled by a factor of 4.
ADAC	EuroTest configuration: sled fixed door
ADAC	Modified EuroTest configuration: intruding door sled crabbed 10° and fixed door.
ADAC	Modified EuroTest configuration: intruding door sled crabbed 10° & intruding door.

In the baseline ISO test configuration shown above, contact between the side intruding door and the CRS starts at approximately 20 ms. Twenty milliseconds later, the dummy starts interacting with the side of the CRS. Up to this moment, the dummy has been

moving laterally until the hip and the shoulder/upper arms contact the shell or padding of the safety seat. Contact between the dummy's head and the side wing of the CRS begins at approximately 60 ms and lasts for only 25 milliseconds. Ninety milliseconds after the start of the simulation, the dummy is moving away from the impact area and at about 100 ms begins interacting in a much more benign way with the opposite side of the CRS.

Figure A1 in Appendix 2 shows a sequence of pictures corresponding to a frontal crash simulation taken at 20 ms intervals. CPU time for the lateral simulations increased with respect to the frontal runs due to the addition of the hinged door, CRS side padding, and corresponding contacts. Typical computation times in the SGI 3800 were: 4.5 hours with 4 processors, 6.5 hours with 2 processors and 9.8 hours (acceptable overnight running time) with 1 processor.

## DISCUSSION OF SIMULATION RESULTS

Tables A2, A3 and A4 in Appendix 1 summarize, the main results of the lateral simulations for the following body regions: head, neck, chest and pelvis. The first conclusion derived from the side impact simulation results is that HIC does not seem to be a problem. This can be attributed to the fact that during the simulations there was no contact between the dummy's head and the intruding hardware.

Chest and head maximum resultant acceleration values are comparable to those obtained during laboratory testing conducted by Paton et al [31]. Most of the chest resultant acceleration values exceed the 55 G's threshold. 65 G's is a typical value for the majority of the simulations. Chest accelerations for simulations without intruding door are in good agreement with results of actual tests such as the ones conducted by Turbell et al [32]. Without an intruding door, the chest accelerations lie in the neighborhood of 30 G's both for simulations and tests.

Axial forces on the neck fall below the injury criteria proposed by NHTSA for the Hybrid III 3-year-old dummy: 2340 N in tension and 2120 N in compression [33]. However, it is worth noting that maximum values are reached not for axial but for lateral forces and so far no injury criteria have been agreed upon for neck lateral forces. An issue of much bigger concern is lateral flexion. All simulation values are far beyond Transport Canada suggested maximum values [34]: 30 Nm for the upper neck and 59 Nm for the lower neck. As pinpointed in the CREST study, neck injuries tend to be very serious

(AIS 3+) and for that reason special attention should be directed to head lateral containment [35, 36].

Very high compression loads were observed at the acetabulum even though the 3ms clip does not capture the short duration but extremely high peak forces. These occur at the beginning of the contact between the dummy's pelvic region and the CRS. Although real-life injury patterns indicate that this region represents only 3% of all the injuries [21], attention to this region is suggested for further research because the CRS FE model does not include padding in this area and the high values may originate in the peculiarities of this model.

When comparing far side or non-struck side to near side (struck) measurements, the tables of results clearly show that all measurements are considerably lower for the case without intruding door (far side). An analogous conclusion can be applied to the simulation where the lateral pulse is removed and the intruding door is maintained (ISO only door case).

The absence of padded areas in the CRS side wing translates into high loads transferred to most of the body regions. Rather surprisingly, head accelerations are higher in the padded vs. the non-padded case. A plausible explanation is that in the padded case the first interaction between the dummy's upper arm and the side wing of the CRS is softer and allows for more interaction between the head and that same area. In other words, loads are distributed over both the arms and the head. In the case of the non-padded CRS, most of the loads are transferred through the dummy's left arm into the chest. Closer examination of the acceleration curves for the head in these two cases clearly shows a higher absolute value of the acceleration for the non-padded case (30 percent higher); however, this pronounced spike is not captured by the 3ms clip. HIC value is, as expected, higher for the case of the non-padded simulation.

With regard to the influence of the US SNCAP longitudinal pulse, except for the head resultant acceleration and the neck lateral bending, the rest of the injury measurements do not show significant changes. The immediate conclusion is that the side impact is the predominant effect in the crash and that the longitudinal pulse, which is about four times less severe in terms of acceleration values, does not significantly increase the injury criteria values. This holds true even when the SNCAP average pulse was scaled by a factor of 2, 3 and even 4.

In order to assess for repeatability of the simulation results, one of the cases (ISO with 214 longitudinal

pulse scaled by a factor of 2) was run with a different number of processors. A remarkable agreement between the two simulations was found.

The consumer information program EuroTest modified in the 2002 ISO proposed test introduced the two following changes: the simulated door was fixed which eliminated its rotation toward the CRS-dummy; the ECE44R bench was crabbed 10° in order to include a forward movement so that in some instances the head could be exposed to impact against the door. As mentioned earlier, crash investigation studies concluded that the intruding door represents one of the major injuring mechanisms during side crashes. For the type of CRS used in this research, simulating a non-intruding door resulted in injury criteria values that are closer to the far-side conditions rather than the near side conditions proposed for the ISO ad-hoc group.

Except from the acetabulum force, the only values that are higher for the crabbed configuration are the neck loads (i.e. neck flexion moment). Again, it should be noted that this conclusion should not be extrapolated to other CRS types. Paton et al also found large differences when comparing New Zealand test results (fixed door configuration) with intruding door test results [31].

It is important to focus on the fact that the EuroTest methodology is aiming at exposing the dummies to contact with the simulated door for all different types of child restraints, including booster seats. On the other hand, it is clear that the reduction in lateral acceleration resulting from a crabbed angle has a significant positive effect on the maximum lateral acceleration in the dummy's head. It is worth noting that longitudinal accelerations imposed in the EuroTest configuration (obtained by means of the 10°-crab angle) are comparable to those in the FMVSS longitudinal pulsed scaled by a factor slightly larger than 2. Another phenomenon arising as the longitudinal pulse is increased was the existence of a second peak in head/chest loads at about 140 ms.

## ACKNOWLEDGMENTS

The National Crash Analysis Center (NCAC) at the George Washington University wishes to thank its sponsors for their continuous support: the Federal Highway Administration (FHWA) and the National Highway Traffic Safety Administration (NHTSA).

## REFERENCES

- [1] Czernakowski W. and Bell R. "A Method to Assess the Effectiveness of Child Restraint Systems." SAE Paper 970499. Warrendale, PA (USA), 1997.
- [2] "MADYMO 3D User's Manual." TNO Road Safety Institute. Delft (The Netherlands), 2000.
- [3] Wismans J., Matha J., Melvin J.W. and Stalnaker R.L. "Child Restraint Evaluation by Experimental and Mathematical Simulation." 23<sup>rd</sup> Stapp Crash Conference. SAE Paper No. 791017. Warrendale PA (USA), 1979.
- [4] Der Avanessian H., Ridella S.A., Mani A. and Drishnaswamy P. "An Analytical Model to Study the Infant Seat Airbag Interaction." SAE Paper No. 920126. Warrendale PA (USA), 1992.
- [5] Nett R. and Appel H. "Child Safety in Small and Micro Cars." 16<sup>th</sup> ESV Conference paper No. 98-S7-W-14. Ontario (Canada), 1998.
- [6] Brewer J.C. "Effects of Angles and Offsets in Crash Simulations of Automobiles with Light Trucks." 17<sup>th</sup> ESV Conference paper No. 308. Amsterdam (The Netherlands), 2001.
- [7] Langwieder K., Hummel T., Lowne R. and Huijskens C. "Side Impact to Children in Cars. Experience from International Accident Analysis and Safety Tests." 15th ESV Conference. Melbourne (Australia), 1996.
- [8] Malm S., Kullgren A., Krafft M., and Ydenius A. "Hurkan vi skydda barn i bil? (How to protect children in cars?)." Seminar "Trafiksäkerhet ur ett Nollvisionsperspektiv", Stockholm (Sweden), 1997.
- [9] Langwieder K. and Hummel T. "Children in Cars – Their Injury Risk and the Influence of Child Protection Systems." 12th ESV Conference. Gothenburg (Sweden), 1989.
- [10] Langwieder K. and Hummel T. "Biomechanical Risk Factors for Children in Cars and Aggravation by Misuse of Restraint Systems." 14th ESV Conference. Munich (Germany), 1994.
- [11] Rattenbury S.J. and Gloyns P.F. "A Population Study of UK Car Accidents in Which Restrained Children were Killed." Child Occupant Protection Conference. San Antonio, Texas (USA), 1993.
- [12] Roy A.P., Hill K.J. and Lowne R.W. "The Performance of Child Restraint Systems in Side Impacts." 12th ESV Conference. Gothenburg (Sweden), 1989.
- [13] Agran P., Winn D. and Dunkle D. "Injuries among 4 to 9 Year Old Restrained Motor Vehicle Occupants by Seat Location and Crash Impact."

American Journal of Disability of Children; 143:1317-1321, 1989.

[14] Thomas P. and Frampton R. "Injury Patterns in Side Collisions – A New Look with Reference to Current Test Methods and Injury Criteria." SAE paper No. 99SC01.

[15] "ISO/TC 22/SC 12/WG 1 N 573. ISO/CD 14646. Road Vehicles-Child Restraint Systems-Side Impact Test Method." Geneva (Switzerland), 2001.

[16] Monclus-Gonzalez J., Eskandarian A., Takatori O. And Morimoto J. "Development of Detailed Finite Element Models of Child Restraint Systems for Occupant Protection". 17<sup>th</sup> ESV Conference paper No. 01-S9-O-126. Amsterdam (The Netherlands), 2001.

[17] "Regulation 44, 03 Series of Amendments: Child Restraint Systems." United Nations Economical Commission for Europe, Geneva (Switzerland), 1995.

[18] "Code of Federal Regulation Title 49 (Transportation) Chapter V (NHTSA, DOT) Part 571-214D, Side Impact Protection."

[19] "AS 1754-2000, Child Restraint Systems for Use in Motor Vehicles; AS 3629-1-1991, Methods of Testing Child Restraints, Part 1, Dynamic Testing; AS 3629-2-1991." Standards Australia – Standards New Zealand. Sidney (Australia), 2000, 1991.

[20] Zaouk B. "Occupant Injury Patterns in Side Crashes." Internal Presentation, FHWA/NHTSA National Crash Analysis Center. Washington, DC (USA), 2000.

[21] Langwieder K., Hell W. and Willson H. "Performance of Child Restraint Systems in Real-Life Lateral Collisions." SAE paper No. 962439. Warrendale, PA (USA), 1996.

[22] SNCAP Reports No. 3226, 3289, 3290, 3383, 3463, 3486, 3504, 3518, 3561, 3564 and 3651. DOT, NHTSA. Washington, DC (USA), 2000-2001.

[23] Eichelberger M., Orzechowski K. and McLaughlin P. "An Analysis of Paediatric Head Injuries." Quarterly CIREN Presentation. Washington DC (USA), 2002.

[24] "Final Economic Assessment NHTSA FMVSS 213, FMVSS 225 Child Restraint Systems; Child Restraint Anchorage Systems." Office of Regulatory Analysis Plans and Policy. DOT, NHTSA. Washington, DC (USA), 1999.

[25] First Technology Safety Systems – FTSS. www.ftss.com.

[26] "LS-DYNA Model of the Hybrid III 32 year old Child Dummy Version 2.3B2. User Manual November 2000." First Technology Safety Systems – FTSS. Plymouth, MI (USA), 2000.

[27] Ove Arup & Partners Detroit Limited. www.arup.com.

[28] Peleska F., Kress R. and Klanner W. "2001 Test Internal Report: Child Restraint Systems." ADAC. Munich (Germany), 2001.

[29] Berliner J., Athey J., Baayoun E., Byrnes K., Elhagediab A., Hultman R., Jensen J., Kim A., Kostyniuk G., Mertz H., J. Prest, Rouhana S., Scherer R. and Xu L. "Comparative Evaluation of the Q3 and Hybrid III 3-Year-Old Dummies in Biofidelity and Static Out-of-Position Airbag Tests." 44<sup>th</sup> Stapp Crash Conference. SAE Paper No. 2000-01-SC03. Warrendale PA (USA), 2000.

[30] Peleska F., Kress R., Bischof K., Klanner W. "2002 Test Internal Report: Child Restraint Systems." ADAC. Munich (Germany), 2002.

[31] Paton I.P., Roy A.P. and Lowne R.W. "Development of a sled side impact test for child restraint systems." 16<sup>th</sup> International Technical Conference on Enhanced Safety of Vehicles. Vol. 3, NHTSA, Washington, DC, 2179-2184, 1998.

[32] Turbell T., Lowne R., Lundell B. and Tingvall C. "ISOFIX – A New Concept of Installing Child Restraints in Cars." SAE paper No. 933085. Warrendale, PA (USA), 1993.

[33] "Notice of Proposed Rule Making (NPRM). 49 CFR Part 571." Docket No. NHTSA-02-11707. RIN 2127-AI34. Federal Motor Vehicle Safety Standards; Child Restraint Systems. DEPARTMENT OF TRANSPORTATION, National Highway Traffic Safety Administration. Washington DC (USA), 2002.

[34] "Recommended Procedures for Evaluating Occupant Injury Risk from Deploying Side Airbags." Prepared by the US Side Airbag Out-of-Position Injury Technical Working Group. Draft May 2000.

[35] Lesire P., Grant R. and Hummel T. "The CREST Project Accident Database." 17<sup>th</sup> ESV Conference paper No. 347. Amsterdam (Holanda), 2001.

[36] Trosseille X., Cassan F. and Schrooten M. "Child Restraint System for Children in Cars – CREST Results." 17<sup>th</sup> ESV Conference paper No. 294. Amsterdam (Holanda), 2001.

## APPENDIX 1. ADDITIONAL TABLES

**Table A1.**  
**Basic statistics of the final FE models**

	CRS	CRS padding	Dummy	Harness	Bench	ISO door	Frontal Sim.	Lateral Sim.
Rig. body merge	-	-	52	-	5	-	57	57
Extra nodes	8	-	16	-	-	2	24	26
Nodal rigid body	7	-	-	3	-	-	10	10
Spotweld	2	-	-	-	-	-	2	2
Joints	2	-	19	2	-	1	23	24
Joint stiffness	-	-	15	-	-	-	15	15
Discrete mass	16	-	9	-	-	4	25	29
Shells	10246	414	6436	449	5366	263	22497	23174
Thick shells	-	-	60	-	-	-	60	60
Solids	1015	828	5495	-	3069	2289	9579	12696
Beams	-	-	153	1	-	-	154	154
Element discrete	-	-	2	-	-	-	2	2
Accelerometer	-	-	8	-	1	-	9	9
Total elements	11261	1242	12154	450	8436	2252	32301	36095
Nodes	10446	1269	11698	594	6618	3252	29356	33877
Parts	20	4	164	5	10	3	199	206

**Table A2.**  
**Head main simulation results for the lateral simulations**

Simulation Title	HIC 36	HIC 15	Head max. resultant acceleration (G's)	Head max. lateral acceleration (G's)
ISO	208	166	54	54
ISO no door	45	23	23	21
ISO only padding	26	26	31	3
ISO no padding	246	160	40	37
ISO 214	207	203	64	55
ISO 214x2	183	140	49	46
ISO 214x2b	186	142	50	46
ISO 214x2 10019	211	189	46	40
ISO 214x2 new harness	179	135	47	43
ISO 214x2 no harness	177	141	40	37
ISO 214x3	188	122	44	36
ISO 214x4	254	171	34	31
ADAC fixed door	57	27	21	18
ADAC intruding	125	83	31	28

**Table A3.**  
**Neck main simulation results for the lateral simulations**

Simulation Title	Neck maximum axial force (N)	Neck maximum lateral force (N)	Neck maximum flexion (Nm)	Neck maximum lateral bending (Nm)
ISO	396	1217	22	81
ISO no door	192	521	14	60
ISO only padding	161	151	14	11
ISO no padding	363	1484	18	112
ISO 214	359	1287	18	99
ISO 214x2	-785	1398	33	94
ISO 214x2b	-791	1402	35	94
ISO 214x2 10019	632	1465	29	93
ISO 214x2 new harness	-783	1406	24	92
ISO 214x2 no harness	210	1443	-14	93
ISO 214x3	-1022	1448	49	88
ISO 214x4	-1223	1393	-27	95
ADAC fixed door	265	676	33	73
ADAC intruding	-696	1213	22	92

**Table A4.**  
**Chest and pelvis main simulation results for the lateral simulations**

Simulation Title	Chest maximum resultant acceleration (G's)	Chest maximum lateral acceleration (G's)	Lower spine maximum resultant acceleration (G's)	Lower spine. maximum lateral acceleration (G's)	Left acetabulum maximum force (N)
ISO	63	59	106	102	-1091
ISO no door	28	28	38	38	-261
ISO only padding	10	8	19	16	-571
ISO no padding	110	105	133	125	-1283
ISO 214	67	58	106	103	-973
ISO 214x2	67	59	102	102	-1590
ISO 214x2b	66	59	107	106	-1717
ISO 214x2 10019	66	58	95	88	-843
ISO 214x2 new harness	66	58	106	104	-1464
ISO 214x2 no harness	63	53	90	83	-623
ISO 214x3	76	64	117	110	-1818
ISO 214x4	105	73	129	110	-1725
ADAC fixed door	31	29	34	31	-693
ADAC intruding	68	56	108	101	-1982

## APPENDIX 2. FRONTAL SIMULATION SEQUENCE OF PICTURES

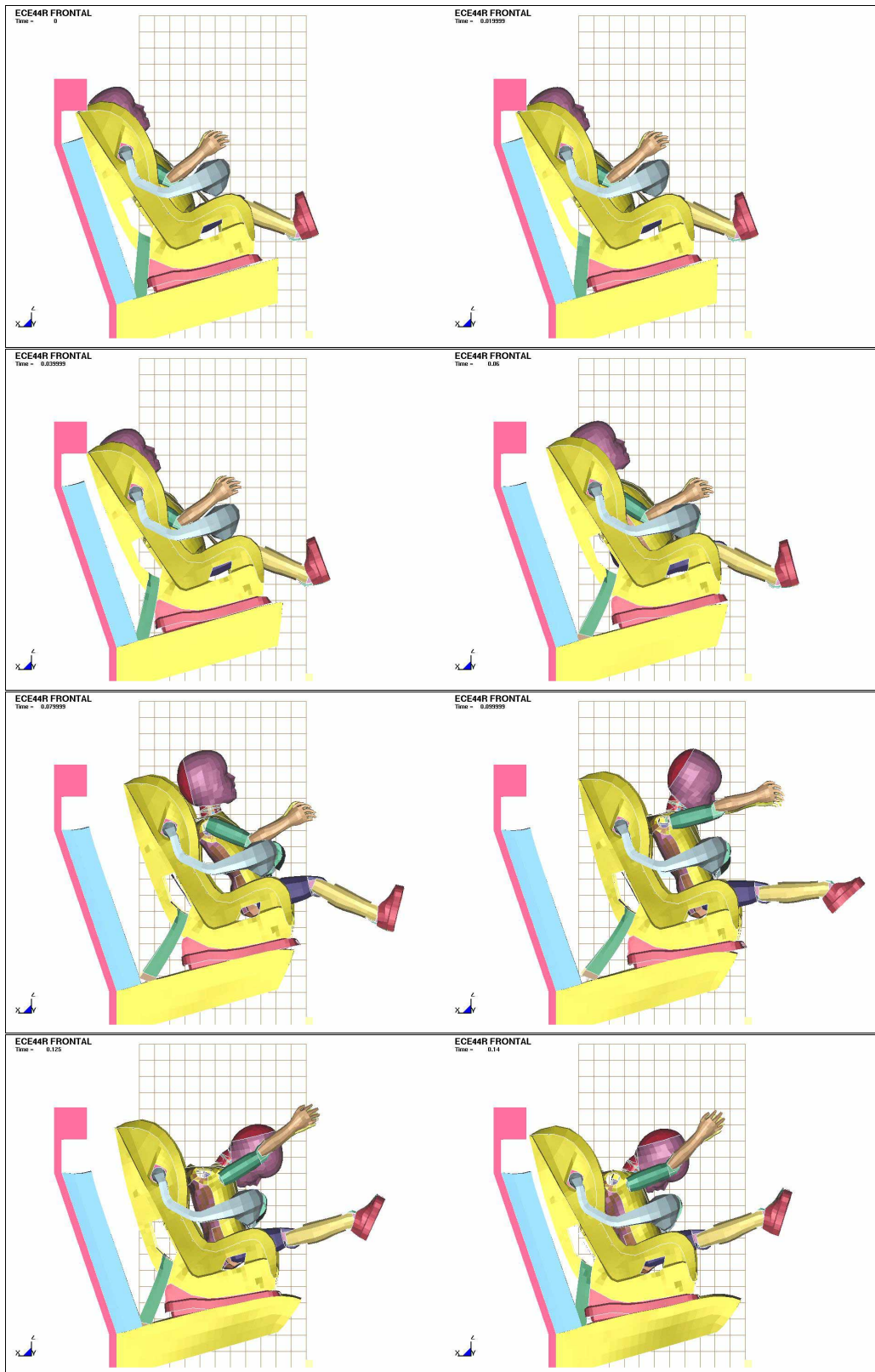


Figure A1. Sequence of pictures during the frontal impact taken at 20 ms intervals.

### APPENDIX 3. LATERAL SIMULATION SEQUENCE OF PICTURES

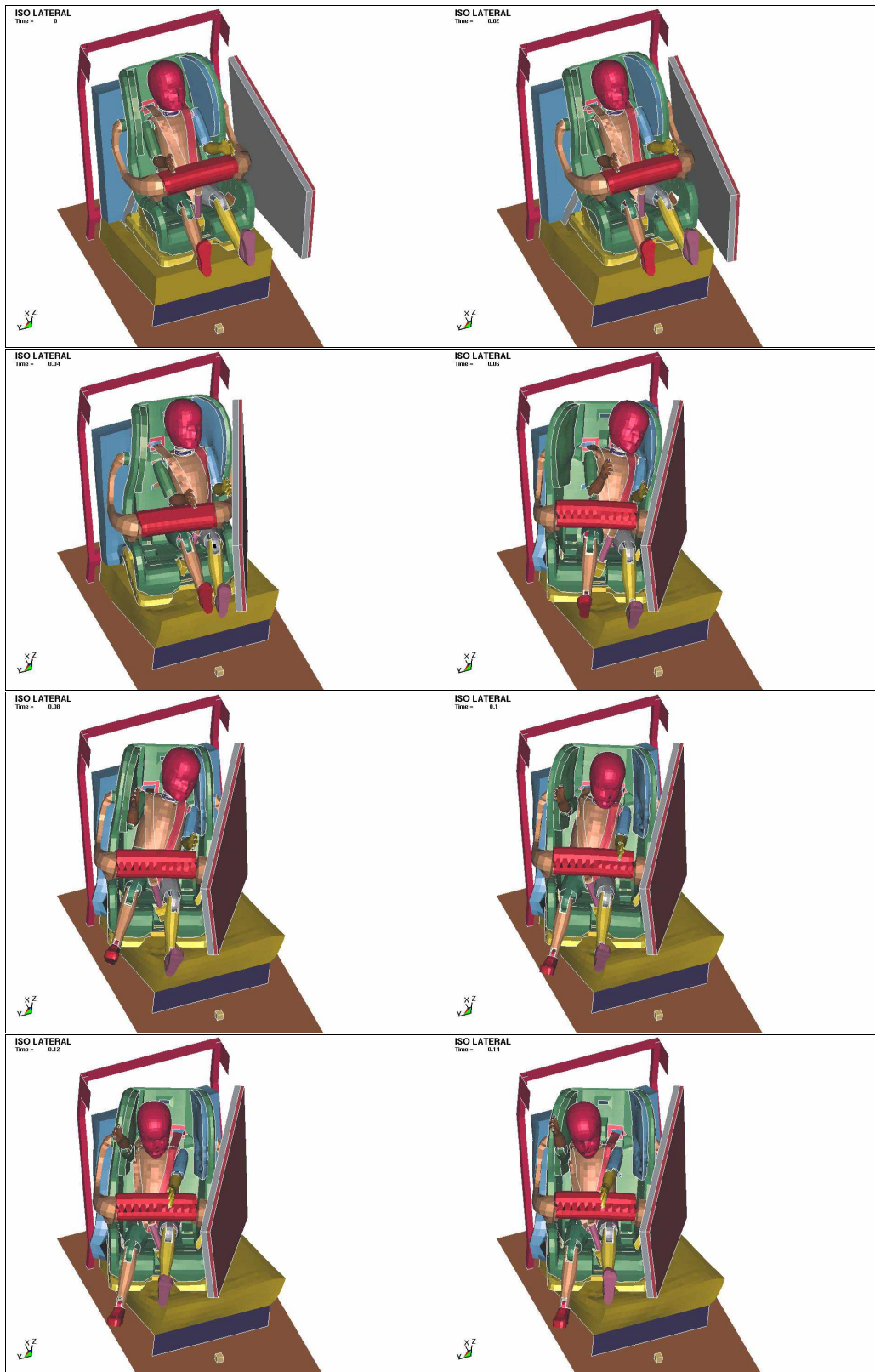


Figure A2. Sequence of pictures during the lateral impact taken at 20 ms intervals.